Cosmic ray propagation in a cylindrical geometry and role of nearby sources in the study of positron excess

Jagdish C. Joshi, Soebur Razzaque
University of Johannesburg, South Africa
E-mail: jjagdish@uj.ac.za, srazzaque@uj.ac.za

Abstract. The flux of positrons observed on Earth produced as secondaries in the cosmic ray nuclei interactions. In the astrophysical scenario positrons are also injected as primaries, and this scenario is very peculiar if these objects are located in the sub-kpc range of solar system. We calculate the positron flux produced by cosmic ray interaction in our Galaxy in a cylindrical geometry, using the DRAGON code, and also check the nearby source contribution using the diffusion-loss equation. In addition to this, we note that an additional population of sources is required for the interpretation of the positron fluxes observed on Earth.

1. Introduction

The satellite detector, Payload for Antimatter Matter Exploration and Light-nuclei Astrophysics (PAMELA) has observed the matter particles (proton, helium and electron) and also the anti-matter particles (antiproton, positron) in the energy range of tens of MeV to hundreds of GeV [1, 2, 3, 4]. Another spectrometer on the international space station, Alpha Magneto Spectrometer (AMS) has also observed these particles in similar energy range [5, 6]. These observations are very significant for understanding the properties of the cosmic ray sources and the properties of the interstellar medium. The discovery of positron excess by PAMELA experiment [7] has been confirmed by Fermi-LAT and AMS experiments [8, 9]. The PAMELA data on positron was taken in 2006-2009, during the minimum solar activity [7]. This excess has been used to understand its origin via dark matter and via astrophysical scenarios [10, 11, 12] and in a recent paper this excess has been associated with the nearby pulsars using HAWC observations [13].

In this work we have used the DRAGON[1] code for the propagation of cosmic rays in the energy range of 100's of MeV to 10's of TeV. We consider their propagation in a cylindrical geometry of radius R and total height H. The R, H parameters are constrained based on the B/C ratio, in the section below. We also consider nearby pulsars as $e^{\pm}$ pair emitters from their pulsar wind nebula (PWN) using the diffusion-loss equation for electrons or positrons [14].

2. Cosmic ray diffusion in our Galaxy and their modelling using DRAGON code

The propagation of cosmic rays in our Galaxy can be modelled by considering the physical processes like, cosmic ray interaction with the gas and radiation field of our Galaxy, scattering of cosmic rays in the regular and turbulent Galactic magnetic field, convection flow of cosmic

[1] The code available at http://www.dragonproject.org/

rays with velocity $\vec{V}$, in Galactic winds, and radioactive decay of cosmic ray nuclei. The equation which describes all these processes is described below [15], and its solution provides us the cosmic ray density per unit momentum $N(\vec{r}, p, t)$.

$$\frac{\partial N}{\partial t} = \vec{\nabla}.(D_{xx}\vec{\nabla}N - \vec{V}N) + \frac{\partial}{\partial p}p^2 D_{pp}\frac{\partial}{\partial p}\frac{1}{p^2}N - \frac{\partial}{\partial p}[\dot{p}N - \frac{p}{3}(\vec{\nabla}.\vec{V})N] - \frac{N}{\tau_f} - \frac{N}{\tau_r} + Q \qquad (1)$$

In this equation D_{xx} takes into consideration the spatial diffusion while D_{pp} is the reacceleration process in the momentum space. The change of moementum with time $\dot{p}$ can have energy gain or loss depending on the astrophysical scenarios. The fragmentation loss is decided by the time scale τ_f while the radioactive loss is included by its decay time τ_r. Q is the source term for cosmic rays from our Galaxy. Cosmic ray propagation through Interstellar medium (ISM) magnetic field leads to scattering and confines them. This scattering decides two main physical mechanism of cosmic rays [16], (i) Escape time of cosmic rays from our Galaxy and their distribution in the ISM, (ii) Energy transfer to the gas, spallation and their reacceleration process in the ISM. The secondary nuclei produced by cosmic ray interactions in our Galaxy provides us the clue about the Galactic matter traversed by cosmic rays in our Galaxy. Based on secondary to primary ratio of cosmic ray nuclei, we can estimate their confinement time in our Galaxy, which is approximately few million years [17, 18].

In the present work we consider diffusion-reacceleration of cosmic ray nuclei and electrons and positrons in our Galaxy in two-dimensional cylindrical model in the energy range 0.1 GeV - 10 TeV. A three-dimensional propagation of cosmic rays in our Galaxy using DRAGON has been discussed earlier [19, 20], and a detailed discussion about this code can be found in the paper by DRAGON group [21]. We have taken the cosmic ray particles are injected into our Galaxy from their sources in a Lorimer distribution [22]. The cosmic ray particles are injected from these sources and scattered in the Galactic magnetic field with disk component $2\mu G$, halo component $4\mu G$ and the turbulent component $7.5\mu G$ respectively [23]. The space and energy dependent diffusion coefficient can be descibed as $D(\rho, z) = \beta^{\eta} D_0(\frac{\rho}{\rho_0})^{\delta} exp(\frac{z}{z_t})$ where ρ is the rigidity of cosmic ray particles. The η index corrects the low energy behaviour of diffusion and z_t the the scale height for the diffusion coefficient.

While cosmic rays travel to us they have to cross the solar medium, where they can be deflected by the solar flare activity. This impact can be modelled with a potential ϕ, which can modify the interstellar cosmic ray spectrum by a factor

$$\epsilon(E_k, Z, A, m_Z) = \frac{(E_k + m_Z)^2 - m_Z^2}{\left(E_k + m_Z + \frac{Z|q|}{A}\phi\right)^2 - m_Z^2}\,, \qquad (2)$$

where E_k is the particle kinetic energy, Z is the atomic number, A is the mass number and m_Z is the nuclear mass.

2.1. Injected cosmic ray spectrum and their diffused spectrum on Earth

The cosmic ray spectrum from their sources follows a power law. If γ_i is the spectral index of the power law and ρ_i is the break in the spectrum then we can list the injected spectrum as shown in our Table 1. Based on our parameters in Table 1 we can fit the B/C ratio, Left panel Figure 1, and the proton, right panel Figure 1, observational data. We can also fit the electron data successfully, left panel of Figure 2, using two breaks in the electron spectrum, where the first break is due to the cooling of electrons in the Galactic magnetic field and the second break might indicate a faster escape of electrons from their sources. A two break electrom spectrum has been also discussed in earlier work [24].

To explain the positron flux we have discussed that we need additional Galactic source population and also some of the nearby pulsars as pair emitters.

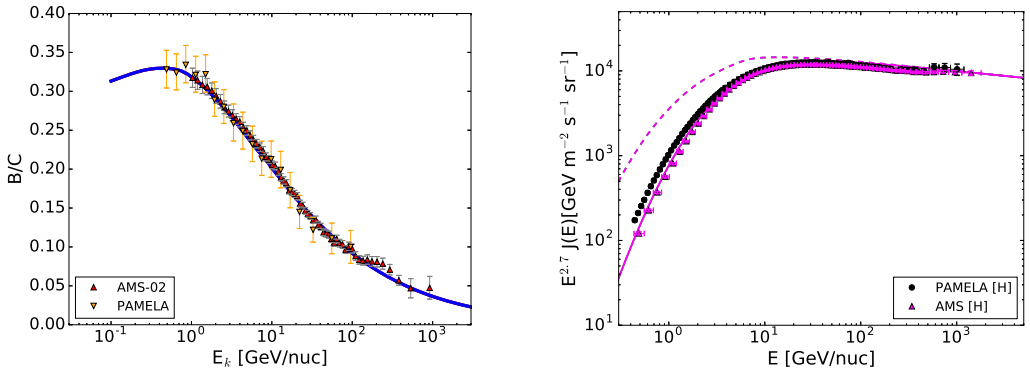

Figure 1: In the left panel B/C ratio calculation using the DRAGON code and plotted against the AMS [6] and PAMELA [25] data. The parameters obtained after fitting this ratio are given in Table 1. In the right panel we show Proton and Helium fluxes plotted against the PAMELA [26] and AMS data [27, 28]. The solid (dashed) lines are fluxes with (without) solar modulation taken into account.

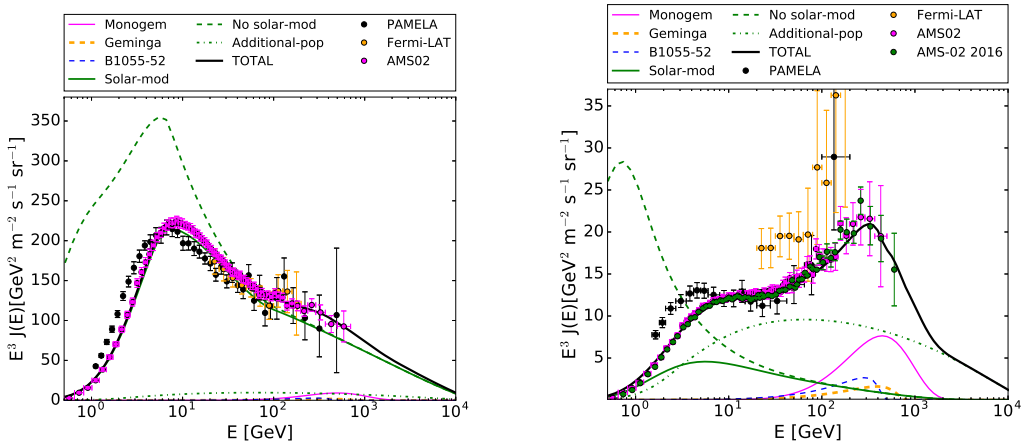

Figure 2: *Left panel:* Electron flux data from PAMELA [2], Fermi-LAT [8] and AMS-02 [29]. *Right panel:* Positron Flux data from PAMELA [7], Fermi-LAT [8] and AMS-02 [29]). Also shown are our model fluxes with black solid line for the total flux in both panels. See main text for more details.

Table 1: Galaxy parameters for a cylindrical halo of radius 12 kpc and height of 8 kpc used in the solution for the transport equation of cosmic rays. All the nuclei follow the same spectrum with a rigidity break at 7.2 GV, the primary electron has two breaks at 6.8 GV and 90 GV and the additional population has a break at 3.8 GV

Parameters	δ	D_0(cm^2/s)	v_A(km/s)	η	$\gamma(p)$	$\gamma(e^-)$	$\gamma(e^\pm)$
Value	0.45	3.0×10^{28}	20	-0.005	2.0/2.37	1.91/2.74/2.45	1.85/2.32

Table 2: Based on pulsar parameters, Monogem, Geminga and B1055-52 dominantly contribute to the electron-positron fluxes in the 100 GeV-1 TeV range in our model.

Name	Dist (kpc)	Age (yr)	Mag-field (G)	P (ms)	$E_{\rm tot}(t)$ (erg)
J0659+1414 (Monogem)	$0.29^{+0.03}_{-0.03}$	1.1×10^5	4.66×10^{12}	384	6.6×10^{47}
J0633+1746 (Geminga)	$0.25^{+0.23}_{-0.08}$	3.42×10^5	1.63×10^{12}	237	5.7×10^{48}
J1057-5226 (B1055-52)	$0.35^{+0.15}_{-0.15}$	5.35×10^5	1.09×10^{12}	197	1.3×10^{49}

3. The nearby pulsars as $e^{\pm}$ pair emitters

Acceleration of charged particles in pulsars can be explained using the polar cap and outer gap models [30, 31]. The accelerated electrons in the pulsar enviroment lose their energy by photon emission and these photons can decay as e^-,e^+ pairs, in the strong pulsar magnetic field [32]. In the high energy region we have taken the contribution from nearby pulsars, shown in Table 2, These pulsar parameters are taken from the Australia Telescope National Facility (ATNF) catalogue[2]. A description of the parameters used in Table 2, is taken from our earlier work [20].

In the energy range above 1 GeV, electrons and positrons loose their energy faster, which limits the distances of these sources w.r.t. an observer on Earth [18]. In Table 2, we have taken sub-kpc pulsars, where Geminga and B1055-52 are the most luminous ones. The injected particle flux from these sources can be taken in the form of power law with an exponential cut-off,

$$Q(E,t,r) = Q_0 \left(\frac{E}{\rm GeV}\right)^{-\Gamma} \exp\left(-\frac{E}{E_c}\right) \delta(t-t_0)\delta(r)\,, \tag{3}$$

where $Q(E,t,r)$ is the cosmic-ray electron (or positron) emissivity, i.e., density per unit energy per unit volume [33]. Also, Q_0 and Γ are normalization and index for the power-law part of the spectrum and $E_{\rm c}$ is an exponential folding energy. A comparison of the amount of spin-down energy going into $e^{\pm}$ pair emissions with the integrated particle injection spectrum, provides the numerical estimation of Q_0. In Eq. (3) t_0 is a time delay for emission and we have considered it 82 kyr for the optimized electron-positron emission from the pulsar-wind nebula (PWN) of a pulsar. The choice of the injection time is based on the fact that PWN emission starts dominating within 100 kyr of the pulsar age [12]. A full discussion on the nearby source calculation using the diffusion-loss equation is discussed in our earlier work [20], please follow it for the explicit calculation.

For an injection time of 82 kyr we need an energy dependent diffusion coefficient, which can be expressed as $10^{27}(E_{\pm}/4.5\ {\rm GeV})^{0.45}$. The estimated flux for Geminga and B1055-42 is shown in the Figure 2, which is more effectively important for the positron flux, as shown in the right panel of Figure 2. In Figure 3 we have plotted the positron excess $e^+/e^+ + e^-$, which is very sensitive to the model parameters. Based on our model we can explain the AMS-02 positron excess data successfully with minute deviation at lower energy due to solar modulations.

4. Summary and conclusion

We have modeled cosmic-ray nuclei and lepton flux data from AMS-02 using a Galactic population of conventional cosmi-ray nuclei and electron sources, a subdominant population of electron-positron sources and nearby pulsars producing electrons and positrons. The cosmic ray nuclei observations by AMS-02 can be explained for a solar modulation potential $\phi = 650$ GV.

[2] `http://www.atnf.csiro.au/people/pulsar/psrcat/`

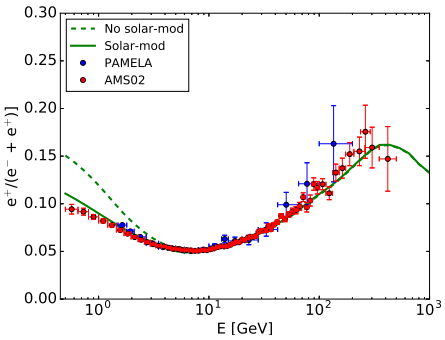

Figure 3: Positron fraction based on our model (solid line) plotted against data from PAMELA [7] and AMS-02 [34].

We have considered the additional population of sources in our Galaxy, whose distribution we have assumed similar to Lorimer distribution, which emit e^- and e^+ and their diffuse spectrum becomes very important in the prospective of positron spectrum. We will explore the origin of this component in our future work. In the discrete source contribution, we found that nearby pulsars Monogem, Geminga and B1055-52 are maximally contributing to the e^- and e^+ fluxes, with 8% and 2% and 4% of spin down energy respectively. The injection spectral index is 1.5 for Monogem and it is 1.4 for Geminga and B1055-52.The exponential folding energy of Monogen is 400 GeV and it is 1 TeV for other two pulsars, which fits the observational data.

References

[1] O. Adriani, G. C. Barbarino, G. A. Bazilevskaya, R. Bellotti, M. Boezio, E. A. Bogomolov et al., *New Measurement of the Antiproton-to-Proton Flux Ratio up to 100 GeV in the Cosmic Radiation*, *Physical Review Letters* **102** (Feb., 2009) 051101.

[2] O. Adriani, G. C. Barbarino, G. A. Bazilevskaya, R. Bellotti, M. Boezio, E. A. Bogomolov et al., *Cosmic-Ray Electron Flux Measured by the PAMELA Experiment between 1 and 625 GeV*, *Physical Review Letters* **106** (May, 2011) 201101.

[3] O. Adriani, G. C. Barbarino, G. A. Bazilevskaya, R. Bellotti, A. Bianco, M. Boezio et al., *Cosmic-Ray Positron Energy Spectrum Measured by PAMELA*, *Physical Review Letters* **111** (Aug., 2013) 081102.

[4] O. Adriani, G. C. Barbarino, G. A. Bazilevskaya, R. Bellotti, M. Boezio, E. A. Bogomolov et al., *Measurement of Boron and Carbon Fluxes in Cosmic Rays with the PAMELA Experiment*, *ApJ* **791** (Aug., 2014) 93.

[5] M. Aguilar, G. Alberti, B. Alpat, A. Alvino, G. Ambrosi, K. Andeen et al., *First Result from the Alpha Magnetic Spectrometer on the International Space Station: Precision Measurement of the Positron Fraction in Primary Cosmic Rays of 0.5-350 GeV*, *Physical Review Letters* **110** (Apr., 2013) 141102.

[6] M. Aguilar, *Precision measurement of the boron to carbon flux ratio in cosmic rays from 1.9 gv to 2.6 tv with the alpha magnetic spectrometer on the international space station*, *Phys. Rev. Lett.* **117** (Nov, 2016) 231102.

[7] O. Adriani, G. C. Barbarino, G. A. Bazilevskaya, R. Bellotti, A. Bianco, M. Boezio et al., *Cosmic-Ray Positron Energy Spectrum Measured by PAMELA*, *Physical Review Letters* **111** (Aug., 2013) 081102.

[8] M. Ackermann, M. Ajello, A. Allafort, W. B. Atwood, L. Baldini, G. Barbiellini et al., *Measurement of Separate Cosmic-Ray Electron and Positron Spectra with the Fermi Large Area Telescope*, *Physical Review Letters* **108** (Jan., 2012) 011103.

[9] AMS Collaboration collaboration, M. Aguilar, G. Alberti, B. Alpat, A. Alvino, G. Ambrosi, K. Andeen et al., *First result from the alpha magnetic spectrometer on the international space station: Precision measurement of the positron fraction in primary cosmic rays of 0.5˘350 gev*, *Phys. Rev. Lett.* **110** (Apr, 2013) 141102.

[10] Y.-Z. Fan, B. Zhang and J. Chang, *Electron/positron Excesses in the Cosmic Ray Spectrum and Possible Interpretations*, *International Journal of Modern Physics D* **19** (Nov., 2010) 2011–2058.

[11] T. A. Porter, R. P. Johnson and P. W. Graham, *Dark Matter Searches with Astroparticle Data*, *ARAA* **49** (Sept., 2011) 155–194.
[12] I. Büsching, O. C. de Jager, M. S. Potgieter and C. Venter, *A Cosmic-Ray Positron Anisotropy due to Two Middle-Aged, Nearby Pulsars?*, *ApJL* **678** (May, 2008) L39.
[13] D. Hooper, I. Cholis, T. Linden and K. Fang, *HAWC Observations Strongly Favor Pulsar Interpretations of the Cosmic-Ray Positron Excess*, *ArXiv e-prints* (Feb., 2017) .
[14] A. M. Atoyan, F. A. Aharonian and H. J. Völk, *Electrons and positrons in the galactic cosmic rays*, *PRD* **52** (Sept., 1995) 3265–3275.
[15] A. W. Strong, I. V. Moskalenko and V. S. Ptuskin, *Cosmic-Ray Propagation and Interactions in the Galaxy*, *Annual Review of Nuclear and Particle Science* **57** (nov, 2007) 285–327.
[16] D. G. Wentzel, *Cosmic-ray propagation in the Galaxy - Collective effects*, *ARAA* **12** (1974) 71–96.
[17] D. Maurin, R. Taillet, F. Donato, P. Salati, A. Barrau and G. Boudoul, *Galactic Cosmic Ray Nuclei as a Tool for Astroparticle Physics*, *ArXiv Astrophysics e-prints* (Dec., 2002) .
[18] V. S. Berezinskii, S. V. Bulanov, V. A. Dogiel and V. S. Ptuskin, *Astrophysics of cosmic rays*. 1990.
[19] D. Gaggero, L. Maccione, D. Grasso, G. Di Bernardo and C. Evoli, *PAMELA and AMS-02 e^+ and e^- spectra are reproduced by three-dimensional cosmic-ray modeling*, *PRD* **89** (Apr., 2014) 083007.
[20] J. C. Joshi and S. Razzaque, *A self-consistent model of cosmic-ray fluxes and positron excess: Roles of nearby pulsars and a sub-dominant source population*, *ArXiv e-prints* (June, 2017) .
[21] C. Evoli, D. Gaggero, A. Vittino, G. Di Bernardo, M. Di Mauro, A. Ligorini et al., *Cosmic-ray propagation with DRAGON2: I. numerical solver and astrophysical ingredients*, *JCAP* **2** (Feb., 2017) 015.
[22] D. R. Lorimer, A. J. Faulkner, A. G. Lyne, R. N. Manchester, M. Kramer, M. A. McLaughlin et al., *The Parkes Multibeam Pulsar Survey - VI. Discovery and timing of 142 pulsars and a Galactic population analysis*, *MNRAS* **372** (Oct., 2006) 777–800.
[23] M. S. Pshirkov, P. G. Tinyakov, P. P. Kronberg and K. J. Newton-McGee, *Deriving the Global Structure of the Galactic Magnetic Field from Faraday Rotation Measures of Extragalactic Sources*, *ApJ* **738** (Sept., 2011) 192.
[24] A. W. Strong, E. Orlando and T. R. Jaffe, *The interstellar cosmic-ray electron spectrum from synchrotron radiation and direct measurements*, *A&A* **534** (Oct., 2011) A54.
[25] O. Adriani, G. C. Barbarino, G. A. Bazilevskaya, R. Bellotti, M. Boezio, E. A. Bogomolov et al., *Measurement of Boron and Carbon Fluxes in Cosmic Rays with the PAMELA Experiment*, *ApJ* **791** (Aug., 2014) 93.
[26] O. Adriani, G. C. Barbarino, G. A. Bazilevskaya, R. Bellotti, M. Boezio, E. A. Bogomolov et al., *PAMELA Measurements of Cosmic-Ray Proton and Helium Spectra*, *Science* **332** (Apr., 2011) 69.
[27] M. Aguilar, D. Aisa, B. Alpat, A. Alvino, G. Ambrosi, K. Andeen et al., *Precision Measurement of the Proton Flux in Primary Cosmic Rays from Rigidity 1 GV to 1.8 TV with the Alpha Magnetic Spectrometer on the International Space Station*, *Physical Review Letters* **114** (May, 2015) 171103.
[28] M. Aguilar, D. Aisa, B. Alpat, A. Alvino, G. Ambrosi, K. Andeen et al., *Precision Measurement of the Helium Flux in Primary Cosmic Rays of Rigidities 1.9 GV to 3 TV with the Alpha Magnetic Spectrometer on the International Space Station*, *Physical Review Letters* **115** (Nov., 2015) 211101.
[29] M. Aguilar, D. Aisa, A. Alvino, G. Ambrosi, K. Andeen, L. Arruda et al., *Electron and Positron Fluxes in Primary Cosmic Rays Measured with the Alpha Magnetic Spectrometer on the International Space Station*, *Physical Review Letters* **113** (Sept., 2014) 121102.
[30] K. S. Cheng, C. Ho and M. Ruderman, *Energetic radiation from rapidly spinning pulsars. I - Outer magnetosphere gaps. II - VELA and Crab*, *ApJ* **300** (Jan., 1986) 500–539.
[31] M. G. Baring, *High-energy emission from pulsars: the polar cap scenario*, *Advances in Space Research* **33** (2004) 552–560.
[32] D. Hooper, P. Blasi and P. Dario Serpico, *Pulsars as the sources of high energy cosmic ray positrons*, *JCAP* **1** (Jan., 2009) 025.
[33] D. Grasso, S. Profumo, A. W. Strong, L. Baldini, R. Bellazzini, E. D. Bloom et al., *On possible interpretations of the high energy electron-positron spectrum measured by the Fermi Large Area Telescope*, *Astroparticle Physics* **32** (Sept., 2009) 140–151.
[34] L. Accardo, M. Aguilar, D. Aisa, A. Alvino, G. Ambrosi, K. Andeen et al., *High Statistics Measurement of the Positron Fraction in Primary Cosmic Rays of 0.5-500 GeV with the Alpha Magnetic Spectrometer on the International Space Station*, *Physical Review Letters* **113** (Sept., 2014) 121101.